

Supplementary Materials for

“Mapping and characterizing eelgrass beds using UAV imagery in Placentia Bay and Trinity Bay, Newfoundland and Labrador, Canada”

by Aaron Sneep, Rodolphe Devillers, Katleen Robert, Arnault Le Bris, and Evan Edinger

### **Supplementary Methods: SegOptim Parameter Space Delineation**

In ArcMap 10.7, the segment mean shift algorithm spectral detail values can range from 1 to 20, spatial details can range from 1 to 20, and minimum segment size specifies the minimum size of a segment, in pixel count. The parameter space was determined through experimentation in ArcMap 10.7 with a subsample of the orthomosaics by setting spatial and spectral detail to the maximum value of 20 and minimum segment size to 20. Experimentation involved decreasing the value of either spectral detail or spatial detail by increments of 1, while keeping the two other parameters constant. When the output segmentation raster exhibited under-segmentation (i.e., multiple image features were contained in one image segment), the previous value was set as the lower limit of the parameter space. These values were 18 and 17 for spectral detail and spatial detail, respectively. The parameter space for minimum segment size was set with a lower limit of 1 and an upper limit of 100. The lower limit of 1 is the most detailed setting and the upper limit of 100 was determined through preliminary tests of the genetic algorithm. The preliminary tests produced optimal minimum segment sizes less than 100, and therefore it was determined that minimum segment sizes from 1 to 100 were a sufficiently large parameter space to contain an optimum solution without being too large as to hinder computation time.

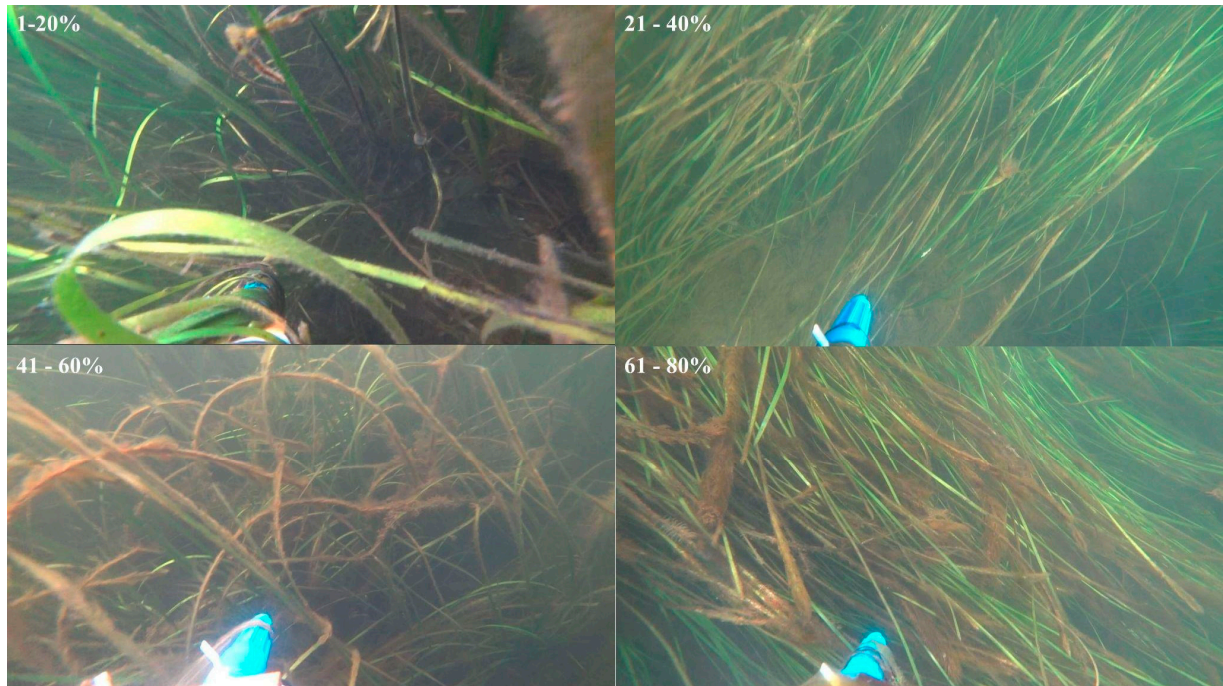


Figure S1. Underwater image examples of epiphyte cover classes observed at the Placentia Swans site. The percent of eelgrass surface in the field of view covered by epiphytes was estimated using six classes: 0%, 1-20%, 21-40%, 41%-60%, 61-80%, and 81-100%. The 81-100% cover category was not observed in the underwater videos.

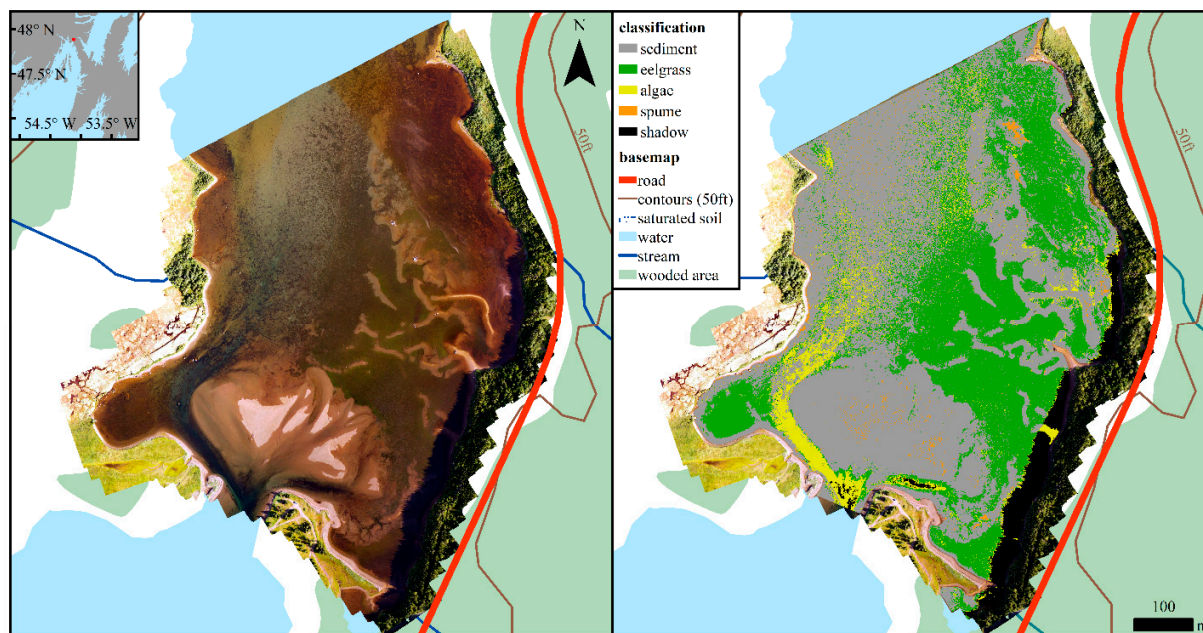


Figure S2. Orthomosaic (left) and thematic map (right) of Come By Chance Gut, NL, CA.

Table S1. Confusion matrix for Come By Chance Gut classification.

		Observed				
Predicted	sediment	94	11	9	6	0
	eelgrass	11	104	7	0	0
	algae	1	2	16	0	2
	spume	2	0	0	4	0
	shadow	0	0	1	0	5

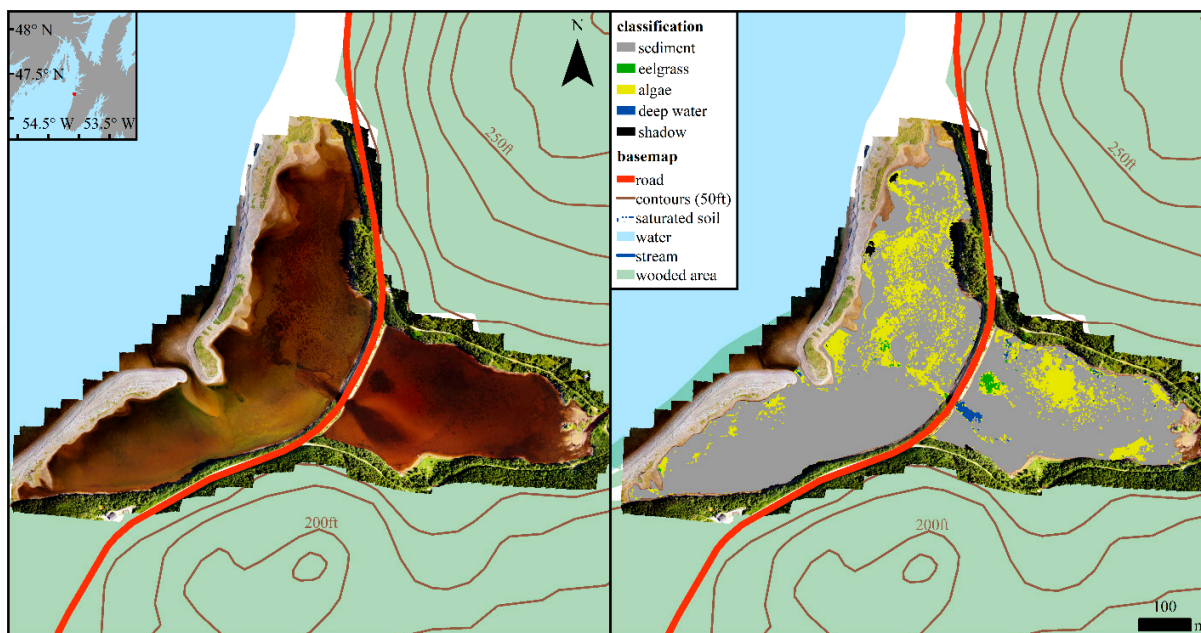


Figure S3. Orthomosaic (left) and thematic map (right) of Glennons Cove Pond, NL, CA.

Table S2. Confusion matrix for Glennons Cove Pond classification

		Observed				
Predicted	sediment	123	0	18	0	1
	eelgrass	0	5	1	0	0
	algae	10	5	41	3	0
	deep water	0	0	3	6	0
	shadow	0	0	0	0	9

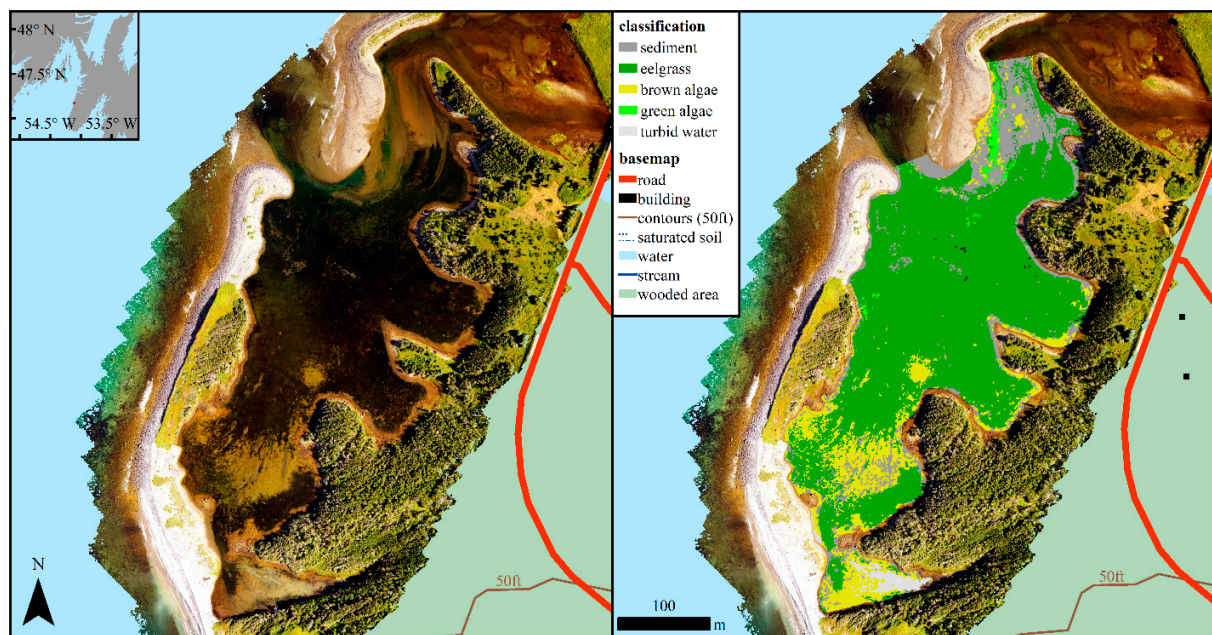


Figure S4. Orthomosaic (left) and thematic map (right) of Great Barasway Pond, NL, CA.

Table S3. Cnfusion matrix for Great Barasway Pond classification.

		Observed					
Predicted		sediment	eelgrass	brown algae	green algae	turbid water	shadow
	sediment	30	1	8	1	1	0
	eelgrass	3	196	2	1	0	6
	brown algae	9	1	35	2	0	0
	green algae	0	0	0	6	0	0
	turbid water	1	0	0	0	9	0
	shadow	0	1	0	0	0	4

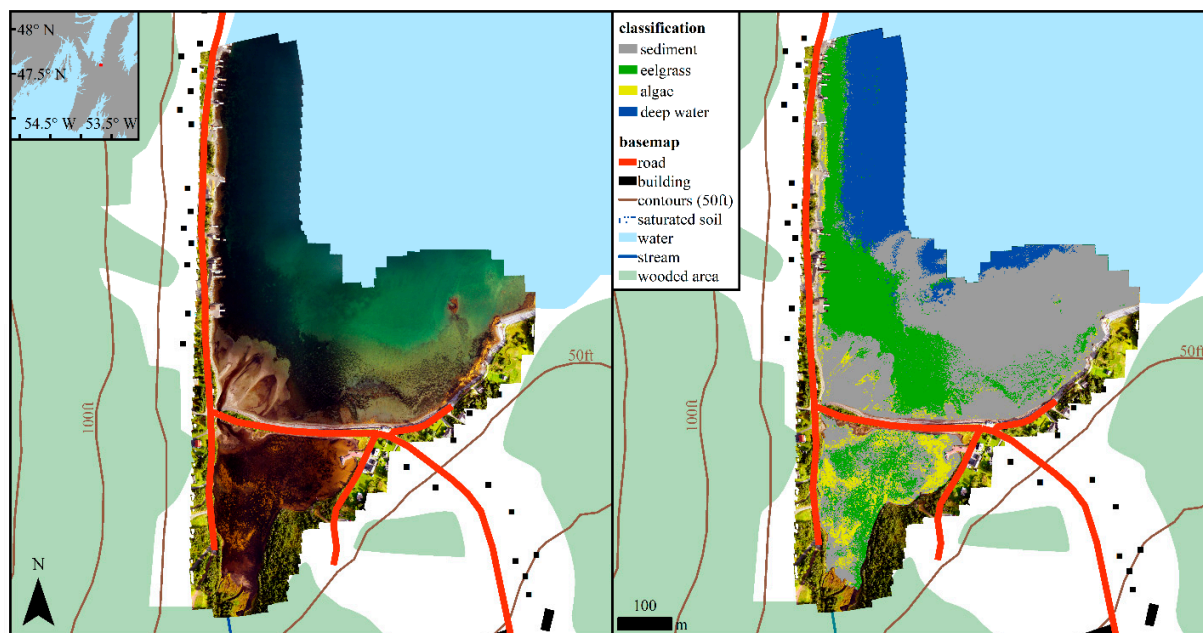


Figure S5. Orthomosaic (left) and thematic map (right) of Old Shop Pond, NL, CA.

Table S4. Confusion matrix for Old Shop Pond classification.

		Observed			
Predicted	sediment	107	8	14	5
	eelgrass	10	83	1	2
	algae	12	2	17	0
	deep water	4	2	0	33

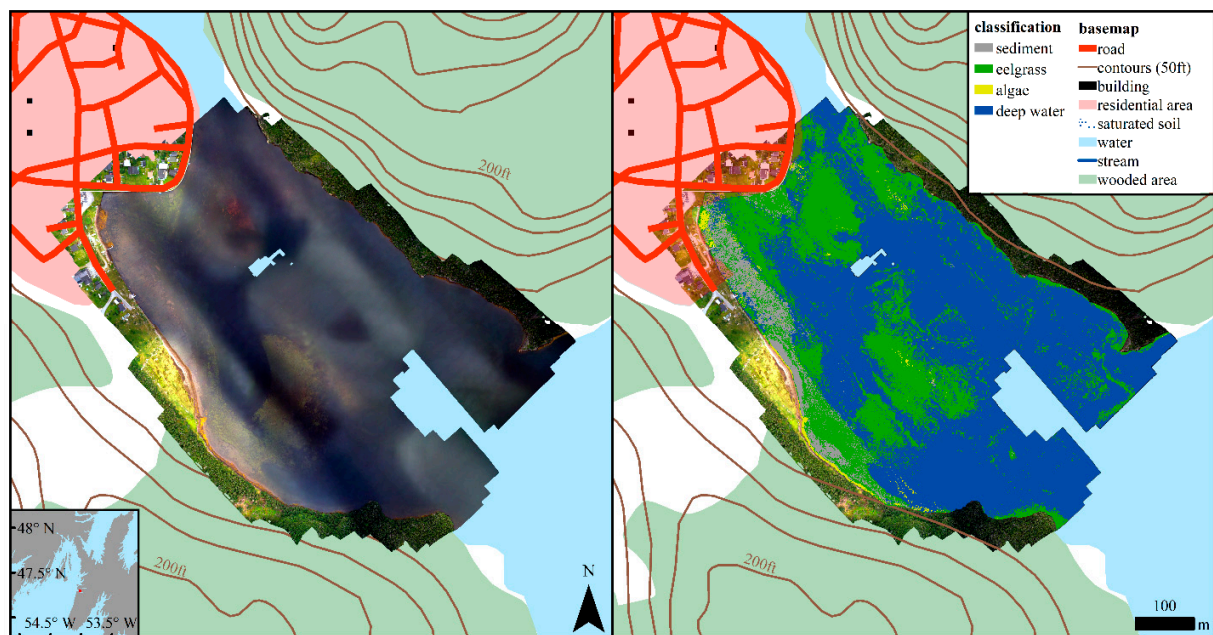


Figure S6. Orthomosaic (left) and thematic map (right) of Placentia Swans, NL, CA.

Table S5. Confusion matrix for Placentia Swans classification.

		Observed			
		sediment	eelgrass	algae	deep water
Predicted	sediment	8	6	3	1
	eelgrass	11	60	4	19
	algae	0	1	5	0
	deep water	2	37	2	141

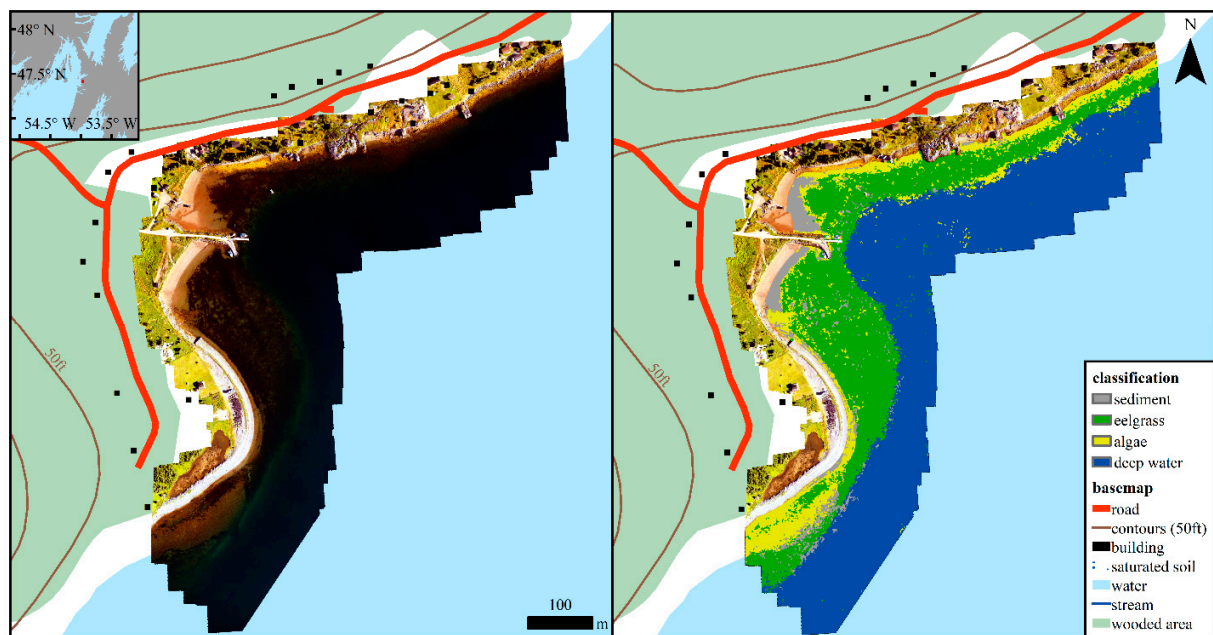


Figure S7. Orthomosaic (left) and thematic map (right) of Ship Harbour, NL, CA.

Table S6. Confusion matrix for Ship Harbour classification.

		Observed			
		sediment	eelgrass	algae	deep water
Predicted	sediment	10	0	3	0
	eelgrass	4	81	20	1
	algae	4	6	22	1
	deep water	5	3	3	134

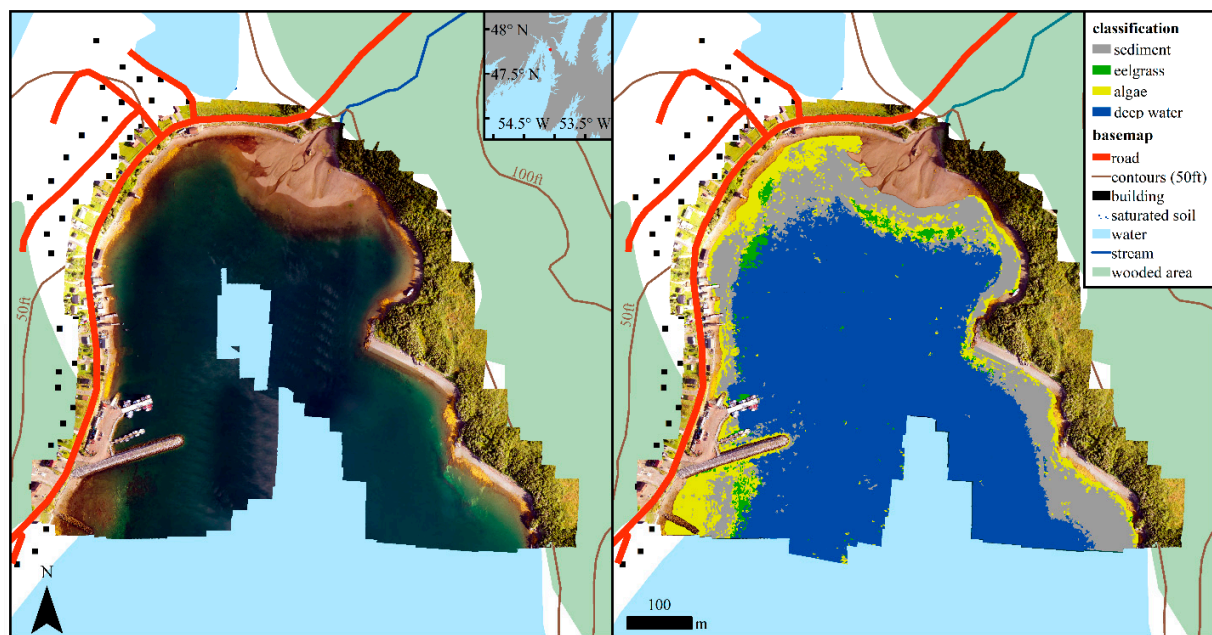


Figure S8. Orthomosaic (left) and thematic map (right) of Southern Harbour, NL, CA.

Table S7. Confusion matrix for Southern Harbour classification.

		Observed			
Predicted		sediment	eelgrass	algae	deep water
	sediment	49	4	15	0
	eelgrass	1	4	6	1
	algae	14	6	24	1
	deep water	10	4	5	153



Figure S9. Orthomosaic (left) and thematic map (right) of Spread Eagle Pond, NL, CA.

Table S8. Confusion matrix for Spread Eagle Pond classification.

		Observed			
		sediment	eelgrass	algae	shells
Predicted	sediment	5	2	3	0
	eelgrass	8	206	15	0
	algae	8	7	44	0
	shells	1	0	0	10



Figure S10. Orthomosaic (left) and thematic map (right) of Frenchmans Island, Sunny Side, NL, CA.

Table S9. Confusion matrix for Frenchmans Island, Sunny Side classification.

		Observed				
Predicted		sediment	eelgrass	algae	deep water	shadow
	sediment	40	9	6	2	0
	eelgrass	19	134	6	3	4
	algae	3	3	1	0	0
	deep water	4	2	0	62	2
	shadow	0	0	0	0	4

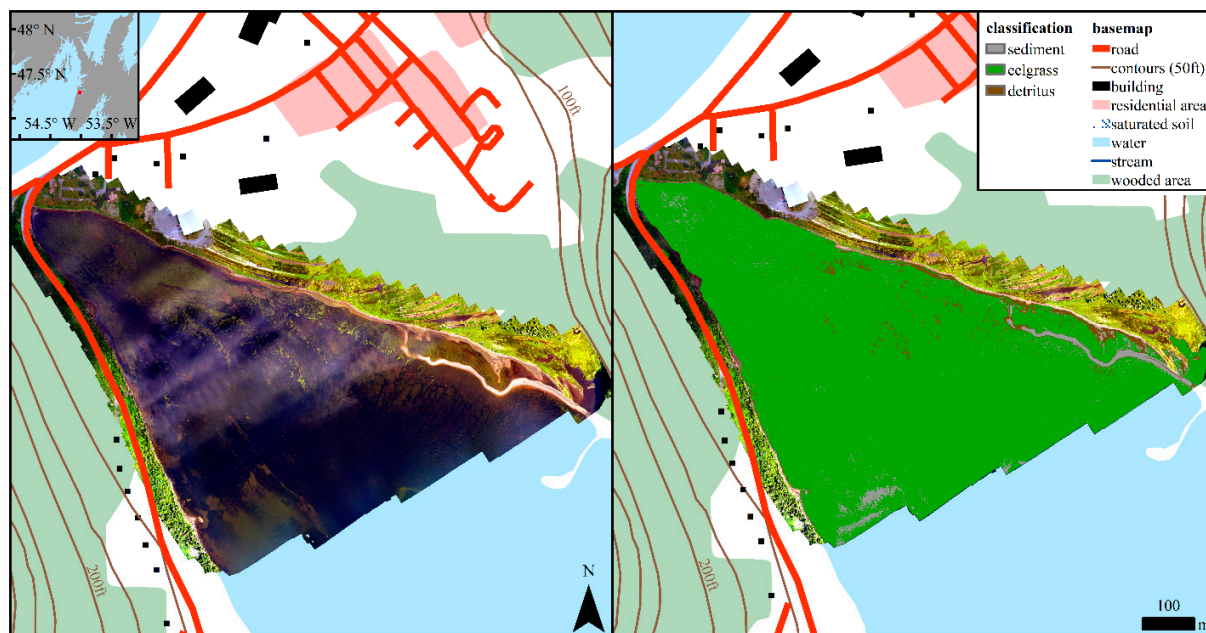


Figure S11. Orthomosaic (left) and thematic map (right) of Western Placentia Southeast Arm, NL, CA.

Table S10. Full confusion matrix for western Placentia Southeast Arm classification.

		Observed		
		sediment	eelgrass	detritus
Predicted	sediment	8	2	1
	eelgrass	18	250	12
	detritus	3	2	4

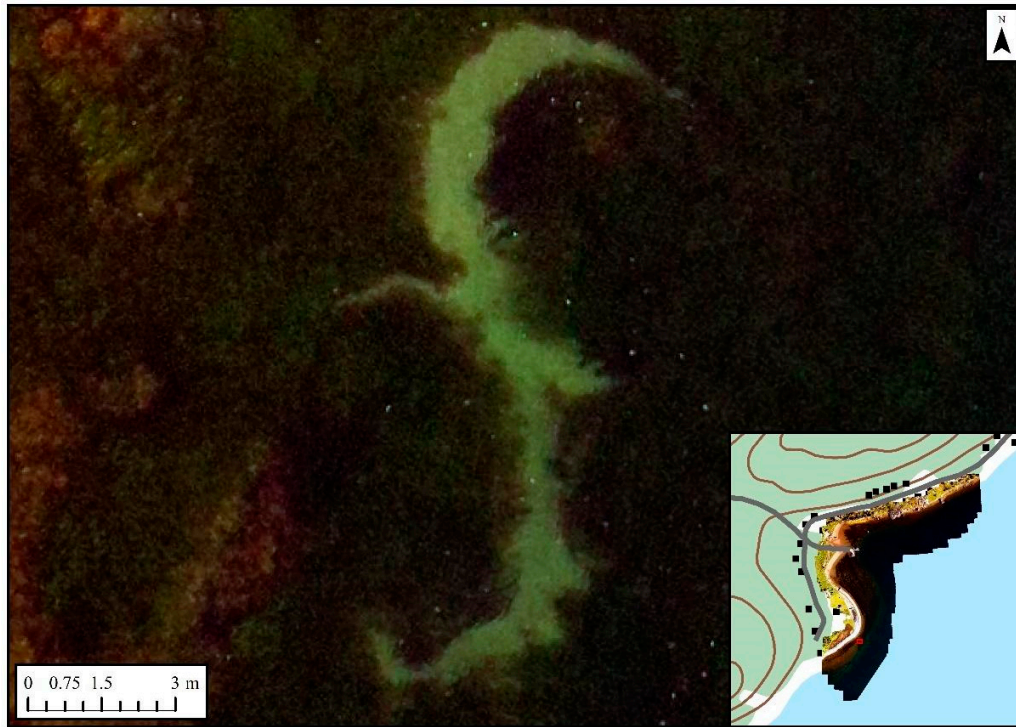


Figure S12. Two semicircular disturbances of an unknown source observed at Ship Harbour. The width of the disturbance is approximately 1 metre. The diameter of the semicircular pattern is approximately 6 metres.

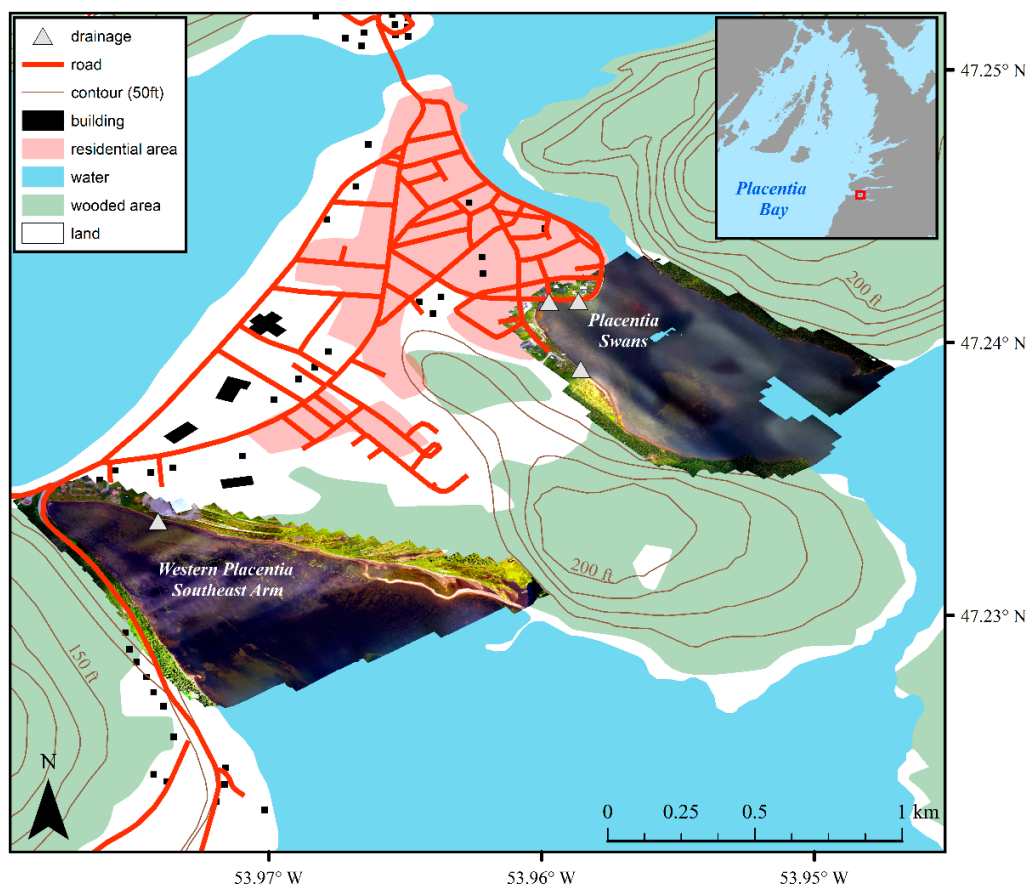


Figure S13. The locations of drainages from the town of Placentia that were observed during field visits to empty into Placentia Swans and western Placentia Southeast Arm.